

S. P. Keller, J. C. Hensel, and F. Stern, CONF-700801 (U. S. AEC Division of Technical Information, Springfield, Va., 1970); J. Stuke, in *Advances in Solid State Physics. Festkörperprobleme IX*, edited by O. Madelung (Pergamon, New York, 1969).

<sup>6</sup>K. Maschke, Ph.D. thesis, University of Marburg, 1970 (unpublished).

<sup>7</sup>L. D. Laude, B. Fitton, and M. Anderegg, *Phys. Rev. Lett.* **26**, 637 (1971).

<sup>8</sup>P. Nielsen, *Bull. Amer. Phys. Soc.* **16**, 349 (1971).

<sup>9</sup>M. R. Barnes and L. D. Laude, to be published.

<sup>10</sup>R. Sandrock, *Phys. Status Solidi (b)* **43**, 199 (1971).

<sup>11</sup>K. Maschke and P. Thomas, *Phys. Status Solidi* **41**, 743 (1970).

## Surface Plasmons and the Reflectivity of *n*-Type InSb†

William E. Anderson and Ralph W. Alexander, Jr.

*Physics Department, University of Missouri—Rolla, Rolla, Missouri 65401*

and

Robert J. Bell

*Physics Department and Graduate Center for Materials Research,  
University of Missouri—Rolla, Rolla, Missouri 65401*

(Received 30 June 1971)

The reflectivity of *n*-type InSb has been measured in the far infrared. The doping of the samples was such that the free-carrier plasma frequency was near the LO mode frequency. The results suggest that samples with a sufficiently thick damage layer show effects due to surface plasmons. Use of a simple model indicates that the surface-plasma excitations are coupled to the phonons.

Surface-plasma excitations were observed by Wood<sup>1</sup> but were not understood until much later. The phenomenon of "Wood's anomalies" was then used by Ritchie to study surface plasmons in Al and Au.<sup>2</sup> Energy loss to surface plasmons by high-energy electrons has been observed for a number of thin metal films. More recently, enhanced photoemission from metals due to surface plasmons has been observed by Spicer and co-workers.<sup>3</sup> Tsui<sup>4</sup> has also observed the interaction of tunneling electrons with surface plasmons in degenerate *n*-type GaAs. Ngai, Economou, and Cohen<sup>5</sup> have provided a theoretical interpretation of Tsui's measurements.

For metals, the surface-plasmon frequency is in the visible, while for degenerate semiconductors this frequency is in the infrared. For example, the surface-plasma frequency for the GaAs samples of Tsui was about 800 cm<sup>-1</sup> (100 meV), considerably above the phonon frequencies in that material. We report reflectivity measurements for Te-doped InSb samples with surface-plasmon frequencies in the 200-cm<sup>-1</sup> range. Thus, the surface-plasmon frequencies lie near the longitudinal optical-phonon frequencies. This considerably complicates the problem since coupling between the surface plasmons and the optical phonons is now possible. Our data, in fact, show that such coupling is important. We shall

use a very simple model in which retardation effects are neglected to explain qualitatively our observations. Of course, retardation effects will be important for the relatively small wave vectors used in our experiments, and a more complete interpretation awaits a theory including the surface-plasmon-optical-phonon coupling and retardation.

The InSb samples were Te doped. Reflectivity measurements were made with three different impurity concentrations such that the free-carrier plasma frequency was in the range 160 to 269 cm<sup>-1</sup>. The plasma frequency  $\omega_p$  is related to the free-carrier concentration by

$$\omega_p^2 = 4\pi Ne^2/m^* \epsilon_\infty. \quad (1)$$

The  $\vec{k}=0$  longitudinal optical phonon of InSb is approximately 190 cm<sup>-1</sup>. A commercial far-infrared Michelson interferometer was used with which the angle of incidence and the polarization of the incident beam could be varied.

Clean, optically polished samples gave results in substantial agreement with published reflectivities.<sup>6</sup> In an attempt to adapt the method used by Ritchie<sup>2</sup> for metals, a grating of 80 lines per cm was cut on all the grating samples. The grating profile was semicircular with 63.5- $\mu$ m-diam grooves separated by 63.5- $\mu$ m uncut strips (see inset on Fig. 1). A spark cutter was used

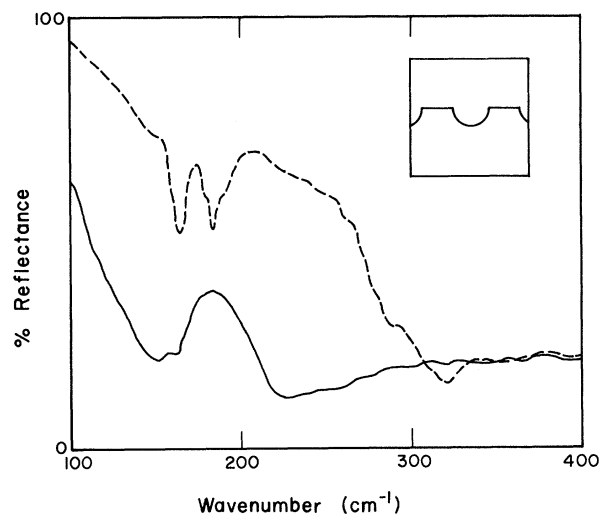


FIG. 1. Percent reflectance of InSb before and after a grating was cut on the surface. The dashed line is for the plane sample and the solid line is for the same sample with a grating cut in it. The sample contained  $3.96 \times 10^{17}$  Te impurities per  $\text{cm}^3$ . The appearance of the additional minimum near the LO phonon frequency is not well understood. The angle of incidence was  $30^\circ$ . Insert: spark-cut-grating profile.

to cut the gratings. For incident radiation polarized with  $\vec{E}$  perpendicular to the grating lines, the photon-surface-plasmon interaction should be enhanced because the grating can provide momentum in multiples of  $2\pi\hbar/d$ , where  $d$  is the grating spacing. We observed the changes in reflectivity shown in Fig. 1 when a grating was cut on the sample, but this change was independent of the polarization of the  $\vec{E}$  of the incident beam. This indicates that we were not successful in reproducing Ritchie's method.

To determine further the effect of the grating, the samples were etched with CP-4 and acetic acid. Successive etching of the spark-cut samples showed a gradual shift of the minima in the reflectivity back to the values of the clean, polished materials as shown in Fig. 2. The reflectance of the samples with gratings returned to that of the uncut samples after about 0.1 mm of material had been etched away. Further etching then produced no change. The removal of 0.1 mm of material produced very little change in the depth of the grating rulings. Thus, the grating itself does not play an important role in our observations. Rather, we have concluded that the spark-cutting operation produced a damage layer upon the sample surface. (The spark-cutting operation involves bombarding the sample with  $\sim 300$ -eV electrons. The local heating vaporized

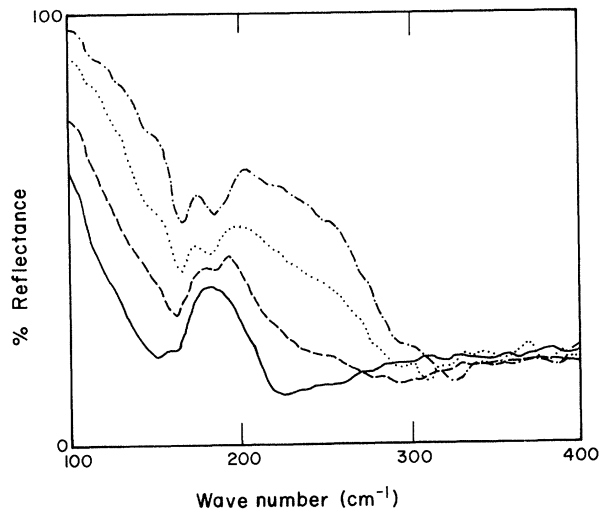


FIG. 2. Percent reflectance of InSb sample with a spark-cut grating surface after successive etches. The sample contained  $3.96 \times 10^{17}$  Te impurities per  $\text{cm}^3$ . Dash-dotted line, 57 sec etch time; dotted line, 12 sec etch time; dashed line, 6 sec etch time; solid line, no etching. The angle of incidence was  $30^\circ$ .

the InSb.)

In this section, we shall use an extremely simple model of a coupled surface-plasmon-optical-phonon system to explain qualitatively the important features of our data. The coupled system of bulk plasmons and longitudinal optical phonons has been theoretically examined by Varga<sup>7</sup> and by Singwi and Tosi.<sup>8</sup> We shall summarize their results with the equation for the frequencies at which the dielectric constant  $\epsilon$  vanishes. These are given by

$$(\omega_{\pm})^2 = \frac{1}{2}(\omega_{LO}^2 + \omega_p^2) \pm \frac{1}{2}[(\omega_{LO}^2 - \omega_p^2)^2 + 4\omega_{LO}^2\omega_p^2(1 - \epsilon_{\infty}/\epsilon_0)]^{1/2}. \quad (2)$$

The minima in reflectivity (where  $\epsilon = 1$ ) lie very near  $\omega_+$  and  $\omega_-$ . The frequency of the  $\vec{k}=0$  LO phonon is  $\omega_{LO}$ , and  $\omega_p$  is the bulk-plasma frequency given by Eq. (1). It has been shown that for a semi-infinite semiconductor bounded by a dielectric, the surface-plasmon frequency is<sup>9</sup>

$$\omega_{SP}^2 = \omega_p^2 / (1 + \epsilon_s / \epsilon_{\infty}). \quad (3)$$

The bounding dielectric medium has dielectric constant  $\epsilon_s$ , and  $\epsilon_{\infty}$  is the high-frequency dielectric constant of the lattice. For InSb ( $\epsilon_{\infty} = 15.68$ ) bounded by a vacuum ( $\epsilon_s = 1$ ), we find

$$\omega_{SP}^2 = \omega_p^2 / (1 + 1/15.68) \approx \omega_p^2. \quad (4)$$

If we assume that instead of being bounded by a vacuum, the plasma is bounded by a thick damaged layer of InSb (so  $\epsilon_s = \epsilon_\infty$ ), then

$$\omega_{SP}^2 = \omega_p^2/2. \tag{5}$$

A similar assumption of a depletion layer was used by Ngai, Economou, and Cohen<sup>5</sup> in explaining the tunneling data of Tsui. In our case, the electron mobility in the damage layer is much less than in the bulk.

With the above results in mind, we return to our measurements. From reflectivity measurements on undoped InSb samples it is known that the high-frequency minimum in the reflectivity is associated with the LO phonon. Because this minimum shifts with the free-electron concentration, the LO phonons must be coupled to the free carriers. This is well understood in the bulk case, and the dependence of the minimum upon the free-carrier concentration is given by Eq. (2).

We now look at a very simple model of two coupled harmonic oscillators. The two oscillators of mass  $m_1$  and  $m_2$  have spring constants  $k_1$  and  $k_2$ , respectively, and are coupled by a third spring with constant  $k_3$ . The frequencies of the normal modes for this system are known to be<sup>10</sup>

$$(\omega_{\pm})^2 = \frac{1}{2}(\omega_1^2 + \omega_2^2) \pm \frac{1}{2}[(\omega_1^2 - \omega_2^2)^2 + 4k_3^2/m_1m_2]^{1/2}, \tag{6}$$

where  $\omega_1^2 = (k_1 + k_3)/m_1$  and with a similar expression for  $\omega_2$ . Comparing Eq. (6) with Eq. (2), we see that for the coupled bulk-plasmon-LO-phonon system, we must make the identifications

$$\omega_1 = \omega_{LO}, \tag{7}$$

$$\omega_2 = \omega_p, \tag{8}$$

$$k_3^2 = k_{LO}k_p(1 - \epsilon_\infty/\epsilon_0). \tag{9}$$

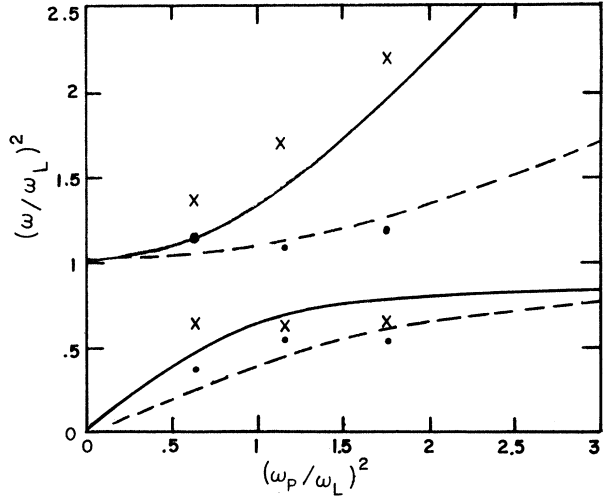


FIG. 3. Frequency of reflectivity minima as a function of free-carrier concentration  $N$ . Solid lines calculated from Eq. (6) for bulk InSb ( $\omega_2 = \omega_p$ ) and dashed lines for grating sample ( $\omega_2 = \omega_p/\sqrt{2}$ ). The crosses indicate experimental values of reflectivity minima for polished (bulk) sample; solid points, same for grating sample. See also Table I.

An effective spring constant for the longitudinal optical phonon is expressible as  $k_{LO}$ , and  $k_p$  is equal to  $m^*\omega_p^2$ . If we now assume that in the process of cutting the grating with a spark cutter a damage layer was created, Eq. (5) shows that the surface-plasmon frequency shifts to  $\omega_{SP} \approx \omega_p/\sqrt{2}$ . Using our simple model, we have assumed a coupled surface-plasmon-phonon system and used Eqs. (7), (8), and (9) with  $\omega_p$  replaced by  $\omega_{SP}$ . Rather reasonable agreement is obtained with the measurements of  $\omega_+$  and  $\omega_-$  and those values predicted by Eq. (6) as shown in Table I and Fig. 3.

The calculated values of  $\omega_+$  and  $\omega_-$  from Eq. (6) in Table I were obtained using the value of  $N$

TABLE I. Experimental and calculated values for  $\omega_+$  and  $\omega_-$  as defined in the text. Calculated values are from Eqs. (6)–(9) using the free-carrier concentration obtained from Hall measurements. The polished samples are labeled “plane” and the same samples with grooves are designated “grating.”

Density of Te impurities ( $10^{17}/\text{cm}^3$ )		$\omega_-$ ( $\text{cm}^{-1}$ )		$\omega_+$ ( $\text{cm}^{-1}$ )	
		Experiment	Theory	Experiment	Theory
1.43	Plane	162	142	237	216
	Grating	125	105	215	207
2.6	Plane	160	170	264	244
	Grating	150	137	212	214
3.96	Plane	165	180	314	284
	Grating	150	159	222	227

from Hall measurements. The calculated frequencies are those for which  $\epsilon = 0$ , while the experimental frequencies are those of the reflectivity minima ( $\epsilon = 1$ ). Hence, the experimentally determined frequencies are not exactly the calculated frequencies. Table I has also been plotted as Fig. 3, showing  $\omega_+$  and  $\omega_-$  as functions of the free-carrier concentration.

To give a shift of the surface-plasmon frequency from  $\omega_p$  to  $\omega_p/\sqrt{2}$ , the depletion layer must be approximately a wavelength thick or thicker. If it is much less than a wavelength thick, the surface-plasmon frequency lies between  $\omega_p$  and  $\omega_p/\sqrt{2}$ . This shift of the plasmon frequency with thickness of the dielectric overcoat has been used by Stanford<sup>11</sup> to study the thickness of AgS films on Ag. Note that our etching data indicate that the depletion layer is of order 0.1 mm thick, or approximately one wavelength thick.

The cutting of the grating also increases the surface roughness and this presumably plays an important role. This is because the incident photon carries less momentum than a surface plasmon of the same energy. However, we are apparently not observing just a change in surface roughness but also a damage layer, because the reflectance minima shift continuously as etching proceeds.

In conclusion we have a very simple model of two coupled harmonic oscillators to explain qualitatively the far-infrared reflectivity of *n*-type InSb. No attempt was made to include retardation effects or to treat rigorously the plasmon-phonon coupling. Clearly, both must be done for a complete treatment. Ngai, Economou, and Cohen<sup>5</sup> have done a calculation (including retarda-

tion) for a semiconductor bounded by a dielectric for the case where the surface-plasma frequency was high enough ( $\sim 800 \text{ cm}^{-1}$ ) so that coupling to the phonons could be neglected. It would be interesting to extend this treatment to include coupling to the phonons. Recently Marschall, Fisher, and Queisser<sup>12</sup> have observed surface plasmons in InSb using the grating technique. The free carrier concentration was an order of magnitude larger than ours, so that the plasma frequency was well removed from the LO phonon frequency and no coupling effects were observed. In addition, their gratings were ruled with a diamond which did not create a damage layer.

†Work supported by the Air Force Office of Scientific Research under Contract No. AFOSR-F-44620-69-C-D122.

<sup>1</sup>R. W. Wood, *Phil. Mag.* **4**, 396 (1902).

<sup>2</sup>R. H. Ritchie, E. T. Arakawa, J. J. Cowan, and R. N. Hamm, *Phys. Rev. Lett.* **21**, 1530 (1968).

<sup>3</sup>J. G. Endriz and W. E. Spicer, *Phys. Rev. Lett.* **24**, 64 (1970).

<sup>4</sup>D. C. Tsui, *Phys. Rev. Lett.* **22**, 293 (1969).

<sup>5</sup>K. L. Ngai, E. N. Economou, and M. H. Cohen, *Phys. Rev. Lett.* **22**, 1375 (1969).

<sup>6</sup>T. J. McMahon and R. J. Bell, *Phys. Rev.* **182**, 526 (1969).

<sup>7</sup>B. B. Varga, *Phys. Rev.* **137**, A1896 (1965).

<sup>8</sup>K. S. Singwi and M. P. Tosi, *Phys. Rev.* **147**, 658 (1966).

<sup>9</sup>E. A. Stern and R. A. Ferrell, *Phys. Rev.* **120**, 130 (1960).

<sup>10</sup>K. R. Symon, *Mechanics* (Addison-Wesley, Reading, Mass., 1964), 2nd ed., p. 190.

<sup>11</sup>J. L. Stanford, *J. Opt. Soc. Amer.* **60**, 49 (1970).

<sup>12</sup>N. Marschall, B. Fischer, and H. J. Queisser, *Phys. Rev. Lett.* **27**, 95 (1971).

## Evidence for One-Dimensional Metallic Behavior in $\text{K}_2\text{Pt}(\text{CN})_4\text{Br}_{0.3} \cdot (\text{H}_2\text{O})_n$

D. Kuse and H. R. Zeller

*Brown Boveri Research Center, CH-5401 Baden, Switzerland*

(Received 27 August 1971)

Single crystals of  $\text{K}_2\text{Pt}(\text{CN})_4\text{Br}_{0.3} \cdot (\text{H}_2\text{O})_n$  show a Drude-type optical reflectivity for light polarized parallel to the crystal axis. The energy of the plasma edge indicates a metallic density of free carriers. The relatively small conductivity at dc and low frequencies and the photoconductivity at 4.2°K can be understood in terms of a simple model assuming metallic strands interrupted by lattice defects.

We report measurements that give for the first time conclusive evidence for the metallic behavior of a square planar organometallic-complex compound.

Planar complexes containing four ligands arranged on the corners of a square around the metal atom have been known for a long time.<sup>1</sup> They form crystals in which the squares are stacked